

IMAGE COMPRESSION USING WAVELET SCALE CORRELATION



by

Lt Col Nisar ul Haq

A thesis submitted to the faculty of Electrical Engineering Department, Military College of Signals, National University of Science & Technology, Rawalpindi in fulfillment of the requirements for the Degree of MS in Electrical Engineering.

Aug 2019

ABSTRACT

With the increasing evolution of technology and digital age, the demand of multimedia products grew faster contributing to the storage of memory devices and insufficient bandwidth and resulted in the need of image compression. The look for effective picture compression strategies is yet a substantial test at the intersection of practical examination and measurements. One of the core advantages of image compression is reduction of redundancy in the image data thus ensuring use of less space in data storage. Discrete wavelet transform is a very competent image compression scheme that results less computational complexity with no sacrifice in image quality. The proposed technique very efficiently compresses the images without deteriorating important details contained in the image where data comprises of multi resolution and multispectral imaging. The aim of this work is to develop an algorithm for image compression without compromising loss of important details contained in the image. An innovative wavelet synthesis approach is conceived based on wavelet scale correlation of the concordant detail bands such that the reconstructed image fabricates a compressed image. An entropy reduction criterion is used in parallel to PSNR for analytical analysis of the results. The subjective analysis supported by the objective analysis reveals that the results image compression through the proposed scheme is satisfactory in various noise environments. Discrete wavelet transform (DWT) using scale correlation is a compression approach that works effectively than the simple wavelet decomposition. Scale multiplication improves the localization accuracy significantly while keeping high detection efficiency.

ACKNOWLEDGMENT

First of all I am thankful to Allah for His kindness and blessing to make this work possible. I would like to extend my sincere gratitude to my worthy supervisor Colonel (Retired) Imran Touqir, Electrical Engineering Department Military College of Signals, NUST who always proved to be highly supportive and helpful. He provided valuable insight and guidance at every step of this research from its inception till its completion. I am also thankful to my guidance committee members Colonel Dr Adil Masood Siddiqui and Lt Col Imad Sarwar Malik for their able guidance throughout the thesis process. Finally, I want to express my deepest appreciation to my family and colleagues for their continuous support and encouragement while completing this study.

Together with, I thank the University administration for providing outstanding environment for research, faculty members of MCS for refining my knowledge.

LIST OF ACRONYMS

Acronym	Meaning
WT	Wavelet Transform
WSC	Wavelet Scale Correlation
DWT	Discrete Wavelet Transform
DFT	Discrete Fourier Transform
IDFT	Inverse Discrete Wavelet Transform
IDWT	Inverse Discrete Fourier Transform
SNR	Signal to Noise Ratio
PSNR	Peak Signal to Noise Ratio
QMF	Quadrature Mirror Filter
DT	Discrete Transform
2D	Two Dimensional

TABLE OF CONTENTS

Topic	Page
INTRODUCTION.....	1
1.1 Background.....	1
1.2 Motivation of Research	1
1.3 Problem Statement	2
1.4 Research Goals	2
1.4.1 Academic Goals	2
1.4.2 Technical Goals	2
1.5 Objectives of Research	3
1.6 Scope of Research.....	3
1.7 Research Contribution.....	3
1.8 Organisation of thesis Document	3
LITERATURE REVIEW.....	4
2.1 Background.....	4
2.2 Image Compression	5
2.3 Wavelets and Image Compression	6
2.3.1 Evolution of Wavelets.....	6
2.4 Short Time Fourier Transform	8
2.5 Continous Time Fourier Transform	9
2.6 Discrete Time Fourier Transform	11
2.7 Multi Resolution Analysis	13

2.8	Implementation of Wavelets	18
2.8.1	Image pyramids.....	18
2.8.2	Subband coding	19
2.8.3	Fast Wavelet transform	23
2.9	Perfect reconstruction in Zee Domain	29
2.10	Wavelets Extension in Higher Dimensions.....	30
WAVELET SYNTHESIS FOR IMAGE COMPRESSION		34
3.1	Introduction	34
3.2	Image Compression Algorithm	34
3.2.1	Wavelet Synthesis.....	35
3.2.2	Thresholding	39
3.2.3	Interpolation	41
3.2.4	Matrix Multiplication.....	41
3.2.5	Computational Complexity.....	41
RESULTS AND ANALYSIS.....		42
4.1	Introduction	42
4.2	Input data	42
4.3	Experimental Results	42
4.3.1	Sample 1	43
4.3.2	Sample 2	44
4.3.3	Sample 3.....	46
4.4	Quality Metric	47
CONCLUSION AND FUTURE WORK		50

5.1 Conclusion 50

5.2 Limitations 51

5.3 Future Work 51

References52

Chapter 1

INTRODUCTION

1.1 Background

Advanced images assume a vital part in day to day life applications, for example, satellite TV, attractive reverberation imaging, PC tomography and in addition zones of research and innovation, for example, topographical data frameworks and stargazing. Informational collections gathered by image sensors are by and large sullied by commotion. Flawed instruments, issues with the information securing process, and meddling regular wonders would all be able to debase the information of intrigue. Along these lines, compression is frequently a vital and the initial step to be taken before the images information is broken down. It is important to apply a productive procedure to make up for such information defilement.

The look for effective image compression strategies is as yet a substantial test at the intersection of practical examination and measurements. Notwithstanding the refinement of late proposed strategies, most calculations have not yet accomplished an attractive level of pertinence. All demonstrate an extraordinary execution when the image is compared to the calculation suppositions yet expel image fine structures in different conditions.

1.2 Motivation of Research

This exploration is planned to build up a novel calculation utilizing wavelet scale correlation which can expel commotion of different kinds from the images. A few variables are spurring this exploration; there is a need of programmed removal of

different kinds of clamour from images without human intervention and utilizing a self-contained compression technique. Research on image compression has been continuing for a long time and got certain accomplishments, however, accomplishing precise compressed image and tidying-up all kind of clamor is still extensively troublesome utilizing a single algorithm.

1.3 Problem Statement

There are numerous image compression strategies both in spatial and transform domain. Every strategy performs exceptionally in removal of image clamour of a specific kind yet neglects to perform when an alternate sort of commotion is experienced. The intention is to build up a novel image compression technique utilizing wavelet scale correlation which can perform satisfactorily on different types of commotion models.

1.4 Research Goal

1.4.1 Academic Goals

To complete the inside and out investigation of discrete wavelet change and wavelets scale relationship with a view to utilize its qualities for image compression, additionally to consider the particular zones in the field of versatile thresholding and insertion methods.

1.4.2 Technical Goals

To build up a calculation which can expel clamor of different kinds from images with least client mediation and greatest conceivable exactness. Corresponding the sub groups of wavelets to get the compressed image.

1.5 Objectives of Research

This exploration is expected for writing survey of the examination work officially done on image compression specially in wavelet change area and then to build up a new technique for image compression which can perform palatably on max sorts of clamor models. In the wake of creating testing the proposed calculation on a few examples of images, on various clamor models to check its precision.

1.6 Scope of Research

This exploration exhibits a calculation in light of wavelets scale correlation to compress gray scale images. To check execution effectiveness, the proposed calculation is tried on a few test images and commotion models and results indicate satisfactory results.

1.7 Research Contributions

This research is helpful for offices which incorporate GIS, satellite imagery and military offices.

1.8 Organization of Thesis Document

Chapter 1 briefly introduces image compression, research background, motivation and problem statement. Goal, objectives, scope of research and finally, research contributions are discussed.

Chapter 2 brief literature review of wavelets and subband coding methods.

Chapter 3 exhibits the proposed algorithm.

Chapter 4 experimental outcomes in light of the proposed calculation and their examination in detail.

Chapter 5 concludes and summarizes the thesis work and outlines some future work that can be carried out in this field.

Chapter 2

LITERATURE REVIEW

2.1 Background

Different image contains different types of noises causing use of more data storage as well as bandwidth, therefore, in order to ensure usage of less space and bandwidth in case of transmission, image compression is done at the very first instance. Commotion may happen in advanced images for various reasons. The signal is usually corrupted by noise [1] which is usually Salt & pepper noise or may be additive noise characterized by Gaussian distribution, Poisson distribution, Rayleigh distribution, Uniform distribution, or their combination. To diminish the impacts of clamor, pre-handling of the image is performed. The pre-preparing can be performed in two ways, filtering the image with a Gaussian function, or by using a smoothing function. The issue with above methodologies is that the ideal outcome may not be acquired by utilizing a fixed operator.

However, in this proposition Gaussian commotion and salt and pepper clamor have been utilized to watch the channel's conduct in the boisterous situation. At whatever point a image is changed over starting with one shape then onto the next, for example, digitizing, transmitting, filtering, and so forth., some type of debasement happens at the yield. Also, no imaging framework, however precise it be, can create a correct copy of the scene. So, images obtained through any securing framework are tainted by an assortment of commotion sources. Commotion alludes to stochastic varieties instead of deterministic bends, for example, shading or absence of core interest. Commotion show

in a image is because of extensive variety of sources e.g. varieties in the finder's affectability, ecological varieties, discrete nature of radiations, transmission or quantization blunders, and so on[1]. It is likewise conceivable to regard unimportant scene points of interest as though they are image commotion, for example, surface reflectance surfaces. The qualities of clamor rely upon its source, as does the administrator which best lessens its belongings. Record image commotion is because of numerous sources including corruption because of maturing, photocopying, or amid information catch, for example, sensor issues in a camera, clean covering the optics or can be grabbed amid a point-to-point transmission of a image. As far as a spatially inspected image, uncorrelated clamor is the irregular dim level varieties with in a image that has no spatial reliance from pixel to pixel. As it were, the dark level of a pixel because of uncorrelated commotion does not rely upon the dim levels of its neighbourhood. The working in this proposal has been finished with the supposition that the clamor is uncorrelated with the spatial directions and the pixel's power esteems.

2.2 Image Compression

The lessening of commotion display in images is an imperative part of image handling. For advanced images, commotion depletion is frequently a required advance for some modern investigating strategies, for example, remote sensing. Segregation of commotion and data in the signal is a not well postured issue. Compression is the way toward diminishing clamor in computerized images and comprises of three phases [1]:

- i. Change the boisterous image to another space, i.e. discover a portrayal, which separate the image from commotion.

ii. Control the coefficients in the new space, i.e. keep the coefficients where SNR is high; diminish the coefficients where SNR is low.

iii. Change the controlled coefficients back to the first space.

Diverse image and signal preparing techniques are utilized to lessen commotion. Spatial separating strategies including linear and non-linear are utilized to diminish uncorrelated clamor.

2.3 Wavelets and Image Compression

The hypothesis of wavelets can be drawn nearer through vector spaces, signal handling or by lifting calculations. The name wavelet suggests that they should incorporate to zero and wave above and underneath the flat hub with smaller help. Wavelets can be considered as capacities that fulfill certain numerical necessities. The greatest pick up with wavelets is that they are limited in recurrence and the space areas all the while, in this manner exhibit stable portrayals in the two areas. WT displays a bargain amongst time and recurrence space. The preferred standpoint they offer for image compression is their capacity to precisely find the discontinuities in the image work. The way that the clamor is only the high recurrence substance of the image have given the reason for the utilization of wavelets for image compression.

2.3.1 Evolution of Wavelets

The street towards the wavelets began with Josef Fourier with his research on Frequency Analysis. The term wavelet was first used by Haar in 1909 and presented minimally upheld Haar wavelet. In any case, it was not seen around then that the

wavelets will be set up so firmly in science, present day material science and designing orders. The specialists in 1930 shaped the exploration bearing [2] from recurrence examination into scale investigation. Paul Levy found that keeping in mind the end goal to examine little and complex points of interest, Haar has more adaptable and favorable premise more than Fourier. Littlewood, Paley, and Stein demonstrated the vitality protection of the signal in space domain drove Davis Mar in 1980 to acquaint a powerful route with utilize the wavelets in Digital Image Processing applications. From that point forward different kinds of wavelet changes have been created and numerous different applications have been found. The continuous wavelet transform (CWT) discovers the greater part of its applications in information investigation where it yields a relative invariant time recurrence portrayal. DWT is in any case, the most prevalent. It has incredible signal compaction properties for some classes of certifiable signs while being computationally extremely proficient. Hence, it has been connected to every specialized field including edge location, image division, pressure, compression, Pattern recognition and numerical integration. The hypothesis of wavelets can be developed from various methodologies. Fourier transform constitutes settled bases with boundless help[1]. It is localized in frequency yet does not give space or time data of the signal. The windowing methodology of Fourier transform known as Short Time Fourier Transform (STFT) is a trade-off between localization of frequency and time.

It does not offer adaptability to application to change the resolution according to prerequisites. Along these lines, it isn't very much adjusted to confine neighborhood singularities. It prompts more broad and adaptable approach in which investigation at various determination and points of interest can be made. A capacity can be examined

by taking its projection on a solitary model capacity along its interpretations and scaling with the end goal that the model capacity complies with certain numerical criteria. This marvel brings about CWT. On the off chance that the said premise work is discretized and afterward the signal is broke down, it is named as discrete time wavelet changes. In the event that the interpretations are number products of two then it brings about surely understood dyadic wavelet change. Another approach depends on multiresolution approach which expresses that any lower dimensional signal can be spoken to by its higher measurement or a higher dimensional signal can be spoken to buy bring down measurement motion along its orthogonal supplement.

The interest of such an approach known as MRA encourages maintenance of auxiliary substance that may go undetected at one determination might be anything but difficult to spot at another. However, wavelets couldn't be successfully utilized till Mallat found that dyadic wavelets can be actualized by channel banks. Execution of wavelets has its underlying foundations in subband coding. In the resulting segments every part of wavelets will be quickly touched and afterward its execution for image compression will be visualized. Toward the finish of the part abusing the wavelet's approximating abilities combined with sharp reaction to commotion by the ordinary edge identifiers, a HED has been detailed.

2.4 Short Time Fourier Transform

Fourier representation of signals is known to be powerful in investigation of stationary occasional signals and not supported for dynamic signals. STFT confines the signal to an interim by increasing it by a settled window work, before doing a Fourier examination

of the item. Rehashing the procedure with interpreted renditions of window work permits limited recurrence data all through the signal to be gotten. Since the window width is same for every one of the frequencies, the measure of confinement stays steady for various frequencies[1]. STFT can be numerically characterized as

$$F(w, t) = \int_{t=-\alpha}^{t=\alpha} f(t)g_{w,t}^*(t)dt \quad (2.1)$$

where

$$g_{w,t} = \omega(t - \tau)e^{j\omega t} \quad (2.2)$$

The capacity $\omega(t)$ is a windowing capacity, the least complex of which is a rectangular window that has a unit esteem over a limited interim and is zero somewhere else.

2.5 Continuous Time Wavelet Transform

As opposed to sinusoidal capacity, a wavelet is a little wave whose vitality is amassed in time. Wavelets [2]–[4] are capacities created from one single capacity called mother wavelet by dilatations and interpretations in time space. A wavelet indicated by $\Psi(t)$ ought to have zero normal esteem and unit vitality.

$$\int_{-\alpha}^{\alpha} \varphi(t)dt = 0 \quad (2.3)$$

$$\int_{-\alpha}^{\alpha} |\varphi(t)|^2 dt = 1 \quad (2.4)$$

This ensures its swaying conduct. The moved and scaled wavelets $\psi(a, b(t))$ can be spoken to as:-

$$\varphi_{a,b} = |a|^{-1/2} \varphi\left(\frac{t-b}{a}\right) \quad (2.5)$$

where a and b are two arbitrary real numbers and represent dilations and translations respectively. The pre-factor $|a|^{-1/2}$ is a normalization constant and responsible to ensure that all scaled functions $|a|^{-\frac{1}{2}} \varphi^*\left(\frac{t}{a}\right)$ with $a \in \mathbb{R}$ have the same energy[5]. Thus the wavelet transform of a signal is computed as a collection of inner products of the signal and translated and scaled versions of a mother wavelet $\psi(t)$ which can be written as

$$\omega_f(a, b) = \langle f, \varphi_{a,b} \rangle \quad (2.6)$$

In view of this definition, the wavelet change of a capacity $f(t)$ can be extended as

$$\omega_f(a, b) = \int_{-\infty}^{\infty} f(t) \varphi_{a,b}^*(t) dt \quad (2.7)$$

Since the examination work $\psi(t)$ is scaled and not balanced like the portion of STFT, a wavelet investigation is regularly called time scale examination instead of time recurrence investigation. For the presence of its backwards[1], the acceptability condition must be met i.e.

$$\int_{-\infty}^{\infty} \frac{|\varphi(\omega)|^2}{|\omega|} d\omega < \infty \quad (2.8)$$

where $\Psi(\omega)$ is the Fourier change of mother wavelet $\Psi(t)$. The backwards change to recreate $f(t)$ from $\omega_f(a, b)$ is spoken to as

$$f(t) = \frac{1}{c} \int_{-\infty}^{\infty} \int_{-\infty}^{\infty} \omega_f(a, b) \varphi_{a,b}(t) da db \quad (2.9)$$

Where

$$c = \int_{-\infty}^{\infty} \frac{|\varphi(\omega)|^2}{|\omega|} d\omega \quad (2.10)$$

$\psi(t)$ is furnished with vanishing minutes, so there must be some capacity say $\varphi(t)$ with non-vanishing mean to such an extent that the previous is the subordinate of later

$$\varphi(t) = \frac{d\varphi(t)}{dt} \quad (2.11)$$

$\Phi(t)$ is called as father wavelet which can be also scaled and interpreted on ceaseless scale with the end goal that the vitality remains solidarity.

$$\varphi_{a,b} = |a|^{-1/2} \varphi\left(\frac{t-b}{a}\right) \quad (2.12)$$

However, the connection amongst father and mother wavelets will be refined in segment 2.7 with the assistance of settled spaces[6].

CWT is profoundly excess and the scales are gone up against genuine hub which is inadmissible for advanced preparing. On the off chance that little scales are taken with whole number interpretation at each scale then it is named as discrete time wavelet change.

2.6 Discrete Time Wavelet Transform

Since image is handled by an advanced figuring machine, it is reasonable to discretize a and b and after that speak to the discrete wavelets in like manner [7]. The by and large refreshing methodology of discretizing a and b is

$$a = a_0^m, m \in \mathbb{Z} \quad (2.13)$$

$$b = nb_0 a_0^m, m \in \mathbb{Z} \quad (2.14)$$

Henceforth the wavelets can be spoken to as

$$\psi_{m,n}(t) = a_0^{-\frac{m}{2}} \psi(a_0^{-m}t - nb_0), \quad m, n \in \mathbb{Z} \quad (2.15)$$

The broadly utilized DWT in signal preparing applications is by discretizing the wavelet on dyadic time scale with the end goal that $a_0 = 2$ and $b_0 = 1$ that is called dyadic wavelet change.

$$\psi_{m,n}(t) = 2^{m/2} \psi(2^{-m}t - n) \quad (2.16)$$

where m and n indicate scale and interpretation parameters individually[1]. The DWT of a capacity f(t) henceforth moves toward becoming[1]

$$\omega_f(m, n) = \langle f, \psi_{m,n} \rangle = \int_{-\infty}^{\infty} f(t) \psi_{m,n}^*(t) dt \quad (2.17)$$

The determination of $\psi(t)$ is made with the end goal that the wavelet premise set $\{\psi_{m,n}\}$ constitute an orthonormal premise. Henceforth the wavelet development of f(t) can be communicated as

$$\hat{f}(t) = \sum_m \sum_n \omega_f(m, n) \Psi_{m,n}(t) \quad (2.18)$$

Condition (2.18) does not get the job done PR and a segment of unique signal is missing which will be abided in the ensuing segments. In the comparable balance, we can broaden discrete adaptation of scaling capacity from (2.12) as under

$$\varphi_{m,n}(t) = 2^{-\frac{m}{2}} \varphi(2^{-m}t - n) \quad (2.19)$$

The vast majority of the signal vitality is gathered in less wavelet coefficients; subsequently, it is additionally named as meager element portrayal.

2.7 Multi Resolution Analysis

MRA presents an efficient way to deal with create the wavelets. The possibility of MRA is to estimate a capacity $f(t)$ at various levels of determination. Two capacities are viewed as: the mother wavelet $\psi(t)$ and the scaling capacity $\phi(t)$. The scaled and interpreted forms of scaling capacity is given by (2.19). For settled m , the arrangement of scaling capacities $\phi_{m,n}(t)$ are orthonormal. MRA depends on chain of command of expanding resolutions of scaling capacities and the wavelet capacities develop as result. By straight mixes of the scaling capacity and its interpretations we can produce an arrangement of capacities to speak to any signal[8]

$$f(t) = \sum_n \alpha_n \phi_{m,n}(t), f(t) \in V_m \quad (2.20)$$

The set [8] of every single such capacity produced by direct mixes of the set $\{\phi_{m,n}(t)\}$ is called traverse of the set, signified by $\text{Span}\{\phi_{m,n}(t)\}$. Presently view V_m as vector space relating to the given set. Expect that the determination increments with expanding m , these vector spaces portray progressive estimate vector spaces

$$V^{-\infty} \subset \dots \subset V^{-3} \subset V^{-2} \subset V^{-1} \subset V^0 \subset V^1 \subset V^2 \subset V^3 \subset \dots \subset V^{\infty}$$

each with determination 2^m Correspondingly

$$\dots \perp W^{-3} \perp W^{-2} \perp W^{-1} \perp W^0 \perp W^1 \perp W^2 \perp W^3 \perp \dots \quad (2.21)$$

The arrangement of subspaces must meet the accompanying criteria so as to be an effective contender for MRA

I. Each space must be contained in the following higher determination space

$$V_m \subset V_{m+1} \dots \forall m \in \mathbb{R} \quad (2.22)$$

II. The association of subspaces is thick in the space of square integrable capacities $L^2(\mathfrak{R})$

$$\overline{UV_m} = L^2(\mathfrak{R}) \quad (2.23)$$

III. The crossing point of the considerable number of spaces is a singleton set containing the each of the zero capacity or zero vector

$$\overline{\cap V_m} = 0 \quad (2.24)$$

IV. Getting a capacity from determination space V_0 by a factor of 2^m outcomes in the higher determination space V_m

$$f(t) \in V_0 \leftrightarrow f(2^m t) \in V_{m \dots m} \in \mathbb{R}^+$$

Or if

$$f(t) \in V_m \leftrightarrow f(2^p t) \in V_{m+p} \dots m, p \in \mathbb{R}^+ \quad (2.25)$$

V. The spaces are move invariant i.e. interpreting a capacity in a determination space does not change the determination

$$f(t) \in V_0 \leftrightarrow f(t - n) \in V_0 \quad (2.26)$$

VI. There exist a set that its whole number decipheres frames an orthonormal premise of V_0

$$\{\varphi(t - n) \in V_0 : n \in \mathbb{Z}\}$$

such that

$$\langle \varphi_m, \varphi_n \rangle = \delta_{mn} = \begin{cases} 0 & m \neq n \\ 1 & m = n \end{cases} \quad (2.27)$$

The principle of MRA is that lower dimensional signs can be carefully spoken to in higher dimensional spaces. As the spaces are settled inside the following higher dimensional space, so the contrast between the two adjoining spaces is the orthogonal supplement of the lower measurement space inside the following higher dimensional space i.e.

$$\langle \varphi_{m,n}, \Psi_{m,k} \rangle = 0 \dots \forall m, n, k \in \mathbb{Z} \quad (2.28)$$

For a space V_m along its orthogonal supplement say W_m will constitute the next higher dimensional space V_{m+1}

$$V_{m+1} = V_m \oplus W_m$$

or on the other hand comparably

$$V_m = V_{m-1} \oplus W_{m-1} \quad (2.29)$$

which can be additionally disintegrated into bring down dimensional spaces alongside their supplements

$$V_m = V_{m-2} \oplus W_{m-2} \oplus W_{m-1} \quad (2.30)$$

$$= V_{m-3} \oplus W_{m-3} \oplus W_{m-2} \oplus W_{m-1} \quad (2.31)$$

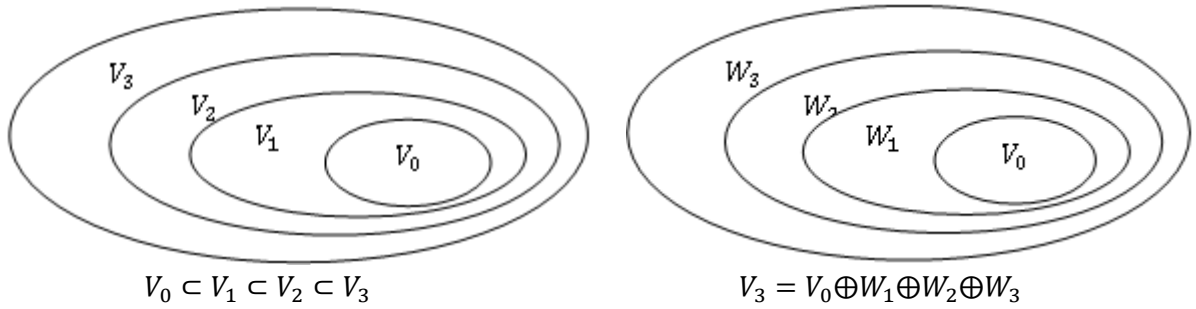


Figure 2.1 Nested spaces. (a) Nested function spaces spanned by scaling functions (b) Relation between scaling and wavelet spaces.

We can express space of all the quantifiable and square indispensable capacities as

$$\mathcal{L}^2(\mathfrak{R}) = V_0 \oplus \sum_{M=0}^{\infty} W_M = V_k \oplus \sum_{p \geq k} W_p \quad (2.32)$$

Or even

$$\mathcal{L}^2(\mathfrak{R}) = \sum_{M=-\infty}^{\infty} W_M \quad (2.33)$$

According to above portrayal of spaces, it is judicious to state that[9]

$$\varphi(t) \in V_0 \Leftrightarrow \varphi(2t) \in V_1 \quad (2.34)$$

which guarantees components in a space are essentially scaled renditions of the components in the following space and if $\varphi(t)$ is in V_0 it is likewise in V_1 spread over by the space $\varphi(2t)$. V_0 and W_0 are the subspaces of V_1 which can be communicated regarding expansion conditions or refinement relations for Haar

$$\varphi(t) = \varphi(2t) + (2t - 1) \quad (2.35)$$

Also

$$\psi t = \varphi 2t - (2t - 1) \quad (2.36)$$

As a rule, $\varphi(t)$ can be communicated as far as weighted whole of moved $\varphi(2t)$ as

$$\varphi(t) = \sum_n h_\varphi(n) \sqrt{2} \varphi(2t - n) \dots n \in \mathbb{Z} \quad (2.37)$$

$\sqrt{2}$ is standardization steady, with comparative thinking and supplemented with Figure 3.1, we find that the wavelets too dwell in the space spread over by the following smaller scaling capacity and can be spoken to by a weighted total of moved scaling capacities

$$\psi(t) = \sum_n h_\psi(n) \sqrt{2} \varphi(2t - n) \dots n \in \mathbb{Z} \quad (2.38)$$

Equation (3.38) builds up that wavelets range the symmetrical supplement spaces and whole number movements are likewise symmetrical, in this way connection between h_φ is upset and adjusted type of h_ψ that can be expressed as

$$h_\psi(n) = (-1)^n h_\varphi(1 - n) \quad (2.39)$$

So far, we built up the idea of settled spaces by which any limited vitality motion in space can be spoken to by straight mix of bases from its subspace along its symmetrical supplements[10]. In the event that $f_{m+1}(t)$ has the goals $m+1$ then it tends to be extended as

$$f_{m+1}(t) = \sum_n \alpha_{m,n} \varphi_{m,n} + \sum_n \beta_m \psi_{m,n} \quad (2.40)$$

Joining (2.37) and (2.38) in (2.40) we can speak to a capacity $f(t) \in V_0$ as

$$f(t) = \sum_n h_\varphi(n) \sqrt{2} \varphi(2t - n) + \sum_n h_\psi(n) \sqrt{2} \varphi(2t - n) \quad (2.41)$$

Equation (3.41) speaks to the total V_o space as its scaled and deciphered variants of the following higher space. Consequently, a signal $f(t)$ can be extended all in all as

$$\begin{aligned} f(t) &= \sum_{m,n \in \mathbb{Z}} \langle f, \psi_{m,n} \rangle \psi_{m,n}(t) \\ &= \sum_{n \in \mathbb{Z}} \langle f, \varphi_{m,n} \rangle \varphi_{m,n}(t) + \sum_{K \leq m, n \in \mathbb{Z}} \langle f, \psi_{k,n} \rangle \varphi_{k,n}(t) \end{aligned} \quad (2.42)$$

Or it can also be written as

$$f(t) = \sum_k \alpha_{j_0}(k) \varphi_{j_0,k}(t) + \sum_{j=j_0}^{\infty} \sum_k \beta_j(k) \psi_{j,k}(t), j_0 \geq k \quad (2.43)$$

Where j_0 is a subjective beginning scale $\alpha_{j_0}(k)$ and $\beta_j(k)$ are called guess and detail coefficients separately which are gotten by taking the inward results of the capacity with scaling and wavelet works as following

$$\alpha_{j_0}(k) = \langle f, \varphi_{j_0,k} \rangle = \int f(t) \varphi_{j_0,k}(t) dt \quad (2.44)$$

Condition (2.43) likewise called wavelet extension arrangement, remakes the first signal without recognizable blunder and fuses the lost bit of $f(t)$ that was missing in (2.18).

$$\beta_j(k) = \langle f, \psi_{j_0,k} \rangle = \int f(t) \psi_{j_0,k}(t) dt \quad (2.45)$$

2.8 Implementation of Wavelets

2.8.1 Image Pyramids

A great deal of likenesses has been found between MRA conditions and image pyramids in which image is decayed into its lower goals making pyramid like image

structure [9]-[10] as appeared in figure 2.2. Expectation leftover is taken at each level so its reverse change exists without blunder. The Image pyramid alongside forecast leftover as delineated in figure 2.3 is undifferentiated from course scale approximations and fine scale points of interest of the wavelets[1].

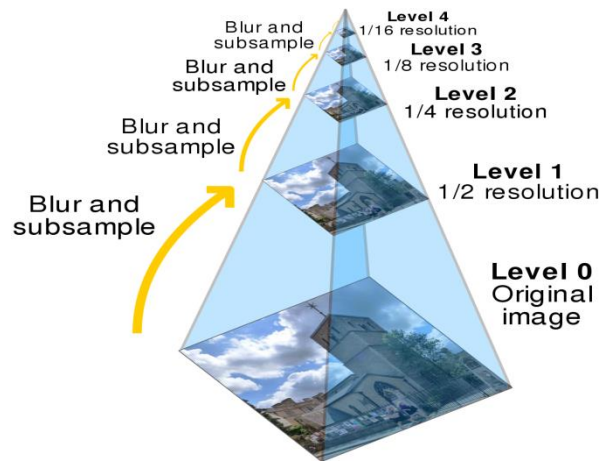


Figure 2.2 Image pyramid

2.8.2 Subband Coding

The wavelets couldn't be adequately actualized in signal handling applications till its linkage with subband coding was investigated. In this plan, the image is deteriorated into an arrangement of band constrained segments, called subbands. The deterioration is performed in a way to such an extent that the disintegrated groups can be reversed back to re-develop the first signal without mistake. The disintegrated signal is destroyed with the end goal that it holds same number of information focuses after pulverization as the first signal. Each decayed band is independently unsampled and sifted so that their mix yields back the first signal or as such the mix of lower dimensional space can produce the following higher dimensional space. For this reason; the exchange capacity

of the framework ought to be solidarity i.e. the union channel bank ought to be the backwards of the investigation channel bank.

$$[L^T \ B^T] \begin{bmatrix} L \\ B \end{bmatrix} = I$$

$$\begin{bmatrix} L \\ B \end{bmatrix} [L^T \ B^T] = \begin{bmatrix} I & 0 \\ 0 & I \end{bmatrix} \quad (2.46)$$

Where L and B mean coefficients of examination channel bank then their transpose comprise coefficients of amalgamation channel bank.

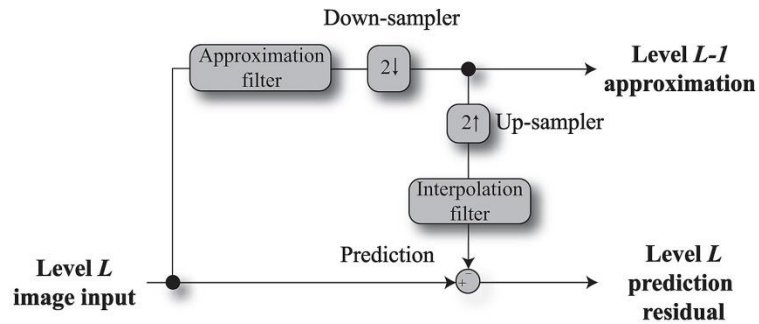


Figure 2.3 Pyramid Implementation

Another approach to state is to factorize solidarity [58] into two components. One factor can relate to coefficients of examination channel bank and the other factor can compare to amalgamation channel bank. Anyway, these components are compelled by certain scientific conditions. There is no set strategy or inductions for finding these elements. The components might be named as enchantment numbers satisfying the scientific conditions, for example, smaller help and symmetry or biorthogonality keeping in mind the end goal to be fruitful possibility for wavelets.

Consider two channel conjugate reproduction channel bank as appeared in Figure 2.4. The investigation channel bank comprises of $h_o[n]$ and $h_1[n]$, is utilized to break the info grouping $f[n]$ into two half-length succession $h_{lp}[n]$ and $h_{hp}[n]$, the subbands that speaks to the information. The $h_o[n]$ and $h_1[n]$ are half band channels whose admired exchange qualities, h_o and h_1 are appeared in figure 2.5 (b). Channel $h_o[n]$ is a lowpass channel whose yield, subband $f_{lp}[n]$, is called a guess of $f[n]$ while $h_1[n]$ is a high pass channel whose yield, subband $f_{hp}[n]$ is called high recurrence or detail some portion of $f[n]$. These channels are control integral and FIR Each band is devastated by of two so the measure of information ought to concur with unique signal. For blend the signal is up examined by a factor of two by embeddings zeros in the middle of back to back examples[11]. At that point it is passed to blend channels independently and afterward consolidated to re-develop the signal.

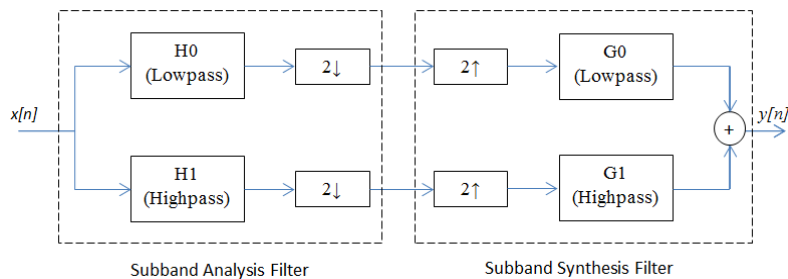


Figure 2.4 Subband coding and synthesis filter bank

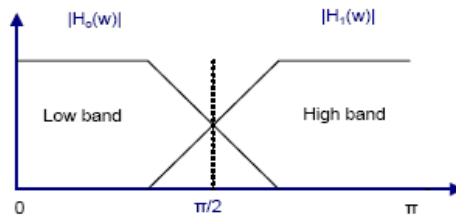


Figure 2.5 Spectrum of half band filters

The objective in subband coding is to choose $h_o[n], h_1[n], g_o[n]$ and $g_1[n]$ so that $f[n] = f[n]$. That is to state that info and yield of subband coding and interpreting framework are indistinguishable.

In all subband coding, union channels are regulated adaptation of the examination channels. One blend channel is being turned around too. For culminate reproduction, the motivation reactions of the blend and examination channels must be connected in one of the accompanying structure[12], [13]

$$g_0[n] = (-1)^n h_1[n] \quad (2.47)$$

$$g_1[n] = (-1)^{n+1} h_0[n] \quad (2.48)$$

Or

$$g_0[n] = (-1)^{n+1} h_1[n] \quad (2.49)$$

$$g_1[n] = (-1)^n h_0[n] \quad (2.50)$$

Channel $h_o[n], h_1[n], g_o[n]$ and $g_1[n]$ in above conditions are said to be cross adjusted on the grounds that askew contradicted channels in Figure 2.4 are connected by regulation. Promote that, they fulfill the under specified biorthogonal condition

$$\langle h_i[2^n - k], g_j[k] \rangle = \delta[i - j] \delta[n], i, j = \{0,1\} \quad (2.51)$$

To grow quick wavelet change we put additionally compels with the end goal that

$$\langle g_i[2^n - k], g_j[n + 2m] \rangle = \delta[i - j] \delta[n], i, j = \{0,1\} \quad (2.52)$$

which characterizes orthonormality for culminate recreation channel banks. Notwithstanding equation above, orthonormal channels can be appeared to fulfill the accompanying two conditions

$$g_1[n] = (-1)^n g_0 [k_e - 1 - n] \quad (2.53)$$

$$h_i[n] = g_i [k_e - 1 - n], i, j = \{0,1\} \quad (2.54)$$

where the subscript k_e is utilized to show that the quantity of channel coefficients must be even. Above conditions demonstrate that amalgamation channel g_1 is identified with g_0 by arrange inversion and balance. What's more both h_1 and h_0 are arrange turned around form of combination channels g_1 and g_0 . Along these lines an orthonormal channel bank can be created around a drive reaction of a solitary channel, called model, the rest of the channels can be processed by utilizing (2.47)- (2.54). Subband coding in the comparative design can be connected to two measurement distinguishable signals by preparing in one measurement taken after by the other measurement which will be examined in the following areas.

2.8.3 Fast wavelet Transform

The wavelets couldn't be adequately utilized [14] found that persistent wavelet premise framed by internal results of orthonormal premise can be executed by a band of consistent Q channels, the non-covering transfer speeds of which contrast by an octave. A ton of likenesses have been found in FWT and subband coding. The high pass $h_1[n]$ a and lowpass $h_0[n]$ utilized in figure 2.4 for subband coding have been utilized reciprocally as $h_\psi[n]$ and $h_\phi[n]$ separately for lucidity where required without the

loss of simplification in the wavelet usage through channel banks. Reexamine (2.37), scaling t by 2^j, deciphering by k, and substituting m=2k+n

$$\begin{aligned}\varphi(2^j x - k) &= \sum_n h_\varphi [n] \sqrt{2} \varphi[2(2^j x - k) - n] \\ &= \sum_m h_\varphi [m - 2k] \sqrt{2} \varphi[2^{j+1} x - m]\end{aligned}\quad (2.55)$$

The scaling vector h_φ can be thought of as the weights used to grow $\varphi(2^j x - k)$ as entirety of scale j+1 scaling capacities. A comparable arrangement of activities on (2.38) yields

$$\psi(2^j x - k) = \sum_m h_\psi [m - 2k] \sqrt{2} \varphi[2^{j+1} x - m] \quad (2.56)$$

Putting the value of $\psi(2^j x - k)$ in (2.45) result

$$\beta_j(k) = \int f(t) 2^{j/2} [\sum_m h_\psi [m - 2k] \sqrt{2} \varphi[2^{j+1} x - m]] dx$$

With a little control of integrals and summation we get

$$\beta_j(k) = \sum_m h_\varphi [m - 2k] \left[\int f(t) 2^{(j+1)/2} \varphi[2^{j+1} x - m] \right] dx \quad (2.57)$$

Consequently, the above condition can be composed as

$$\beta_j(k) = \sum_m h_\varphi [m - 2k] \alpha_{j+1} (m) \quad (2.58)$$

The detail coefficients at scale j are elements of the estimation coefficients at scale j+1.

In comparative mold the wavelet arrangement extension guesses coefficients yield

$$\alpha_j (k) = \sum_m h_\varphi [m - 2k] \alpha_{j+1} (m) \quad (2.59)$$

Whenever $f(t)$ is discrete, the wavelet arrangement extension coefficients progress toward becoming DWT coefficients $W_\psi(j, k)$ and $W_\phi(j, k)$ which can be extended demonstrating connection between DWT coefficients with adjoining scales.

$$W_\psi(j, k) = \sum_m h_\psi[m - 2k]W_\psi(j + 1, k) \quad (2.60)$$

$$W_\phi(j, k) = \sum_m h_\phi[m - 2k]W_\phi(j + 1, k) \quad (2.61)$$

Equation (2.58) and (2.59) uncovers that higher dimensional signal can be disintegrated into bring down dimensional signal. The scale and detail coefficients of higher dimensional space can be computed by arrange switched scaling and wavelet vectors $h_\psi[n]$ and $h_\phi[n]$ afterward destruction by two is like examination bank as portrayed in figure 3.6 [14] with expansion that $\bar{h}_\psi[n] = h_\psi[-n]$ and $h_\phi[n] = h_\phi[-n]$.

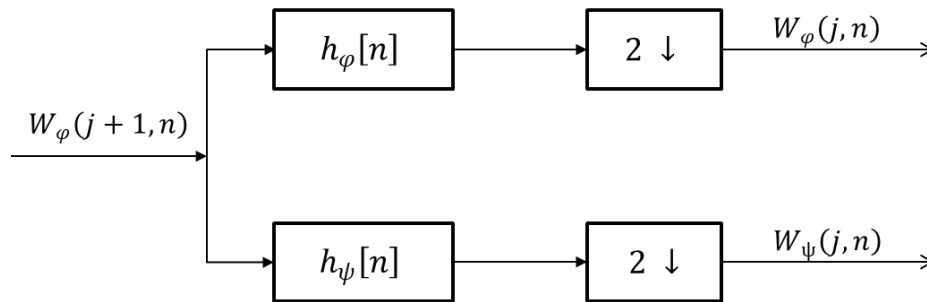


figure 2.6 FWT analysis filter bank

Or on the other hand can be likened as convolutions of $W_\phi(j + 1)$ with $h_\psi[n]$ and $h_\phi[n]$ then crushed by a factor of two yields[1]

$$W_\psi(j, k) = h_\psi[-n] * W_\phi(j + 1, n) \Big|_{n=2k, n} \quad (2.62)$$

$$W_\varphi(j, k) = h_\varphi[-n] * W_\varphi(j + 1, n) \Big|_{n=2k, n} \quad (2.63)$$

Above conditions are the characterizing conditions of FWT. The channel banks appeared in going before chart can be iterated to yield multistage structures for processing DWT coefficients at least two progressive scales

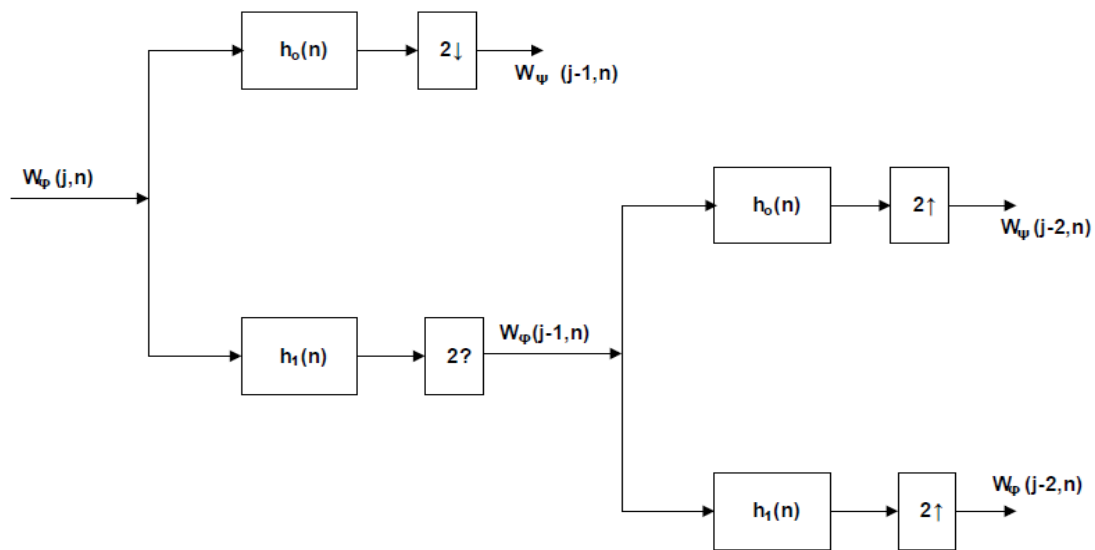


Figure 2.7 Two-dimensional four band filter bank for subband coding

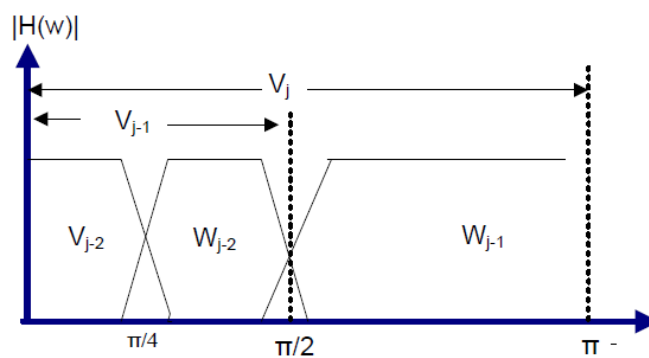


Figure 2.8 Spectrum splitting of the bands

The above chart demonstrates the emphasis of $W_\psi(j)$ part to next goals into $W_\psi(j - 1)$ and $W_\phi(j - 1)$. The scaling capacity is again subjected to same lowpass and high pass channels yielding $W_\psi(j - 2)$ and $W_\phi(j - 2)$. Subsequently $W_\psi(j - 2)$ can additionally part into scaling and wavelet work in next lower measurement. The procedure can be iterated to any phase according to utilization of the application. Anyway, the non-disintegration of information when it spans to zenith is paltry. The range of the capacity according to their goals is delineated in figure 2.8.

The opposite wavelet change is straightforward and the channel coefficients for converse change are computed through (2.47)- (2.54). The scaling and wavelet vectors utilized in forward change, together with level j estimate and detail coefficients produce the level $j+1$ guess coefficients. The state of request inversion of channel coefficients must be considered for symmetrical channel banks. Anyway, for biorthogonal channel banks the investigation and combination channel ought to be cross balanced according to (2.53)- (2.54), which must be fulfilled[15].

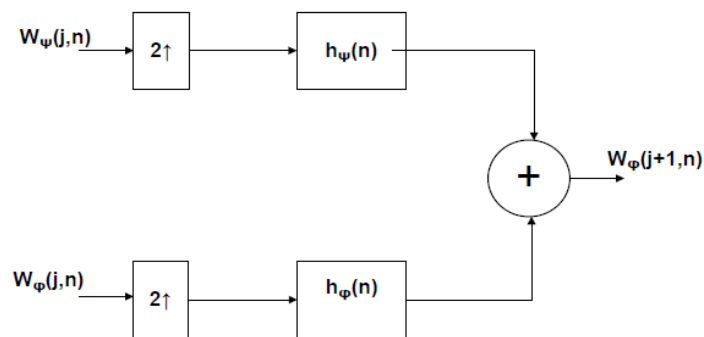


figure 2-9 IFFT synthesis filter bank

The usage of figure 2.9 can be worked out as:-

$$W_\psi(j+1, k) = h_\psi(k) * W_\psi^{2\uparrow}(j, k) + h_\psi(k) * W_\psi^{2\uparrow}(j, k) \Big|_{k \geq 0} \quad (2.64)$$

where $\psi^{2\uparrow}$ connotes up testing by two with the goal that it returns to unique goals. The up inspected coefficients are sifted with $h_\psi[n]$ and $h_\psi[n]$ afterward added to produce a higher scale estimate. The coefficients joining process as portrayed in above figure can be broadened up to any level gave the goals is above single point. A two-phase reverse FWT for Figure 3.7 is appeared beneath which ensures culminate development.

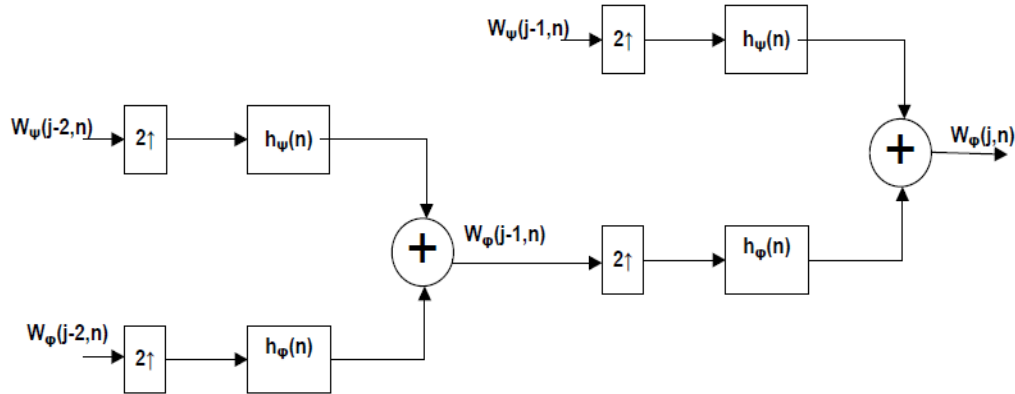


figure (2.10) Two scale inverse IFFT synthesis filter bank

The presence of FWT relies on the accessibility of a scaling capacity for the wavelets being utilized, and also the symmetry or bi symmetry of the scaling capacity and relating wavelets. On the off chance that these conditions are not met like Mexican Hat wavelets which does not have a buddy scaling capacity, can't be actualized in channel banks.

2.9 Perfect Reconstruction in Zee Domain

In Zee domain the conditions for consummate recreation [58], considering figure 2.4, can be built up as

$$\hat{F}(Z) = \frac{1}{2} G_0(Z) [H_0(Z)F(Z) - H_0(-Z)F(-Z)] + \frac{1}{2} G_1(Z) [H_1(Z)F(Z) - H_1(-Z)F(-Z)] \quad (2.65)$$

Rearranging the terms

$$\hat{F}(Z) = \frac{1}{2} [H_0(Z)G_0(Z) - H_1(Z)G_1(Z)] F(Z) + \frac{1}{2} [H_0(-Z)G_0(Z) - H_1(-Z)G_1(Z)] F(-Z) \quad (2.66)$$

The above conditions feature the way that for PR the associating impact because of down sampling and afterward up sampling, the channel reactions must be to such an extent that these drop the associating impacts of one another i.e.

$$H_0(-Z)G_0(Z) - H_1(-Z)G_1(Z) = 0 \quad (2.67)$$

To wipe out the adequacy bending impacts, under said must be fulfilled

$$H_0(Z)G_0(Z) - H_1(Z)G_1(Z) = 2 \quad (2.68)$$

These equations can be simplified into matrix equations as[13]

$$\begin{bmatrix} G_0(Z) & G_1(Z) \end{bmatrix} \begin{bmatrix} H_0(Z) & H_0(-Z) \\ H_0(Z) & H_0(-Z) \end{bmatrix} = \begin{bmatrix} 2 & 0 \end{bmatrix} \quad (2.69)$$

Where examination adjustment matrix is

$$H_m(Z) = \begin{bmatrix} H_0(Z) & H_0(-Z) \\ H_0(Z) & H_0(-Z) \end{bmatrix} \quad (2.70)$$

$$\begin{bmatrix} G_0(Z) \\ G_1(Z) \end{bmatrix} = \frac{2}{\det(H_m(Z))} \begin{bmatrix} H_1(-Z) \\ -H_0(-Z) \end{bmatrix} \quad (2.71)$$

The above network condition ensures PR and the outcomes are in accordance with the time space examination clarifying symmetry conditions in (2.47)- (2.52). Above

conditions can likewise exhibit biorthogonality conditions by taking the item channel of lowpass and high pass as $P(z)$ [1]

$$P(z) = G_o(Z)H_o(Z) = \frac{2}{\det(H_m(Z))} H_o(Z)H_1(Z) \quad (2.72)$$

Also

$$G_1(Z)H_1(Z) = \frac{-2}{\det(H_m(Z))} H_o(-Z)H_1(Z) = P(-z) \quad (2.73)$$

or

$$G_1(Z)H_1(Z) = P(-z) = G_o(-Z)H_o(-Z) \quad (2.74)$$

Therefore

$$G_o(Z)H_o(Z) + G_o(-Z)H_o(-Z) = 2 \quad (2.75)$$

By putting values, we get

$$P(z) + P(-z) = 2 \quad (2.76)$$

Converse Zee change of (3.76) supplements the biorthogonality state of the channels expressed in (47)- (50) for PR of the first signal.

2.10 Wavelet's Extension in Higher Dimensions

One dimensional change can be effectively reached out to two measurements gave [1] that the signal must be distinct i.e. sifting and down inspecting can be connected in one measurement taken after by the other measurement. For images, a two-dimensional scaling capacity $\varphi(x, y)$ and three two dimensional wavelets, $\psi^1(x, y)$, $\psi^2(x, y)$ and $\psi^3(x, y)$ are required. Each capacity is the result of detachable two one dimensional capacities and distinguishable directional wavelets.

$$\varphi(x, y) = \varphi(x)\varphi(y) \quad (2.77)$$

$$\psi^1(x, y) = \psi(x)\varphi(y) \quad (2.78)$$

$$\psi^2(x, y) = \varphi(x)\psi(y) \quad (2.79)$$

$$\psi^3(x, y) = \psi(x)\psi(y) \quad (2.80)$$

Condition (2.77) ascertains the estimation and remaining conditions figure directional varieties. Conditions (2.78), (2.79) and (2.80) give variety along flat, vertical and inclining bearings individually. Two dimensional wavelets can be basically reached out from one dimensional wavelet as

$$\varphi_{j,m,n}(x, y) = 2^{j/2}\psi(2^jx - m, 2^jy - n) \quad (2.81)$$

$$\psi_{j,m,n}^i(x, y) = 2^{j/2}\psi^i(2^jx - m, 2^jy - n), i = 1,2,3 \quad (2.82)$$

where list $i=1,2,3$ shows the directional wavelets i.e. flat, vertical and inclining. The DWT of image $f(x, y)$ of size $M \times N$ is

$$W_\varphi(j_0, m, n) = \frac{1}{\sqrt{MN}} \sum_{X=0}^{M-1} \sum_{Y=0}^{N-1} f(x, y) \varphi_{j_0,m,n}(x, y) \quad (2.83)$$

$$W_\psi^i(j, m, n) = \frac{1}{\sqrt{MN}} \sum_{X=0}^{M-1} \sum_{Y=0}^{N-1} f(x, y) W_{i,m,n}^j(x, y), i = \{H, V, D\} \quad (2.84)$$

As in one dimensional case, j_0 is a subjective beginning scale and $W_\varphi(j_0, m, n)$ coefficients characterize an estimate of $f(x, y)$ at scale j_0 . The $W_\psi^i(j, m, n)$ coefficients include level, vertical and corner to corner points of interest for

scales $j \geq j_0$. Normally $j_0=0$ and $N=M=2^j$ for $j=0,1,2,3,\dots, j-1$ and $m=n=0,1,2,\dots, 2^{j-1}$ is taken.

The opposite two-dimensional DWT can be gotten by

$$f(x, y) = \frac{1}{\sqrt{MN}} \sum_{X=0}^{M-1} \sum_{Y=0}^{N-1} W_{\varphi}(j_0, m, n) \varphi_{j_0, m, n}(x, y) + \frac{1}{\sqrt{MN}} \sum_{i=H,V,D} \sum_{J=j_0}^{\infty} \sum_m \sum_n W_{\psi}^i(j, m, n) \psi_{j, m, n}^i(x, y) \quad (2.85)$$

Two-dimensional distinguishable scaling and wavelet capacities can be actualized by essentially taking the one-dimensional FWT of the lines of $f(x, y)$ trailed by one dimensional FWT of the subsequent sections. Figure 2.11 demonstrates the square outline of the channel banks[1].

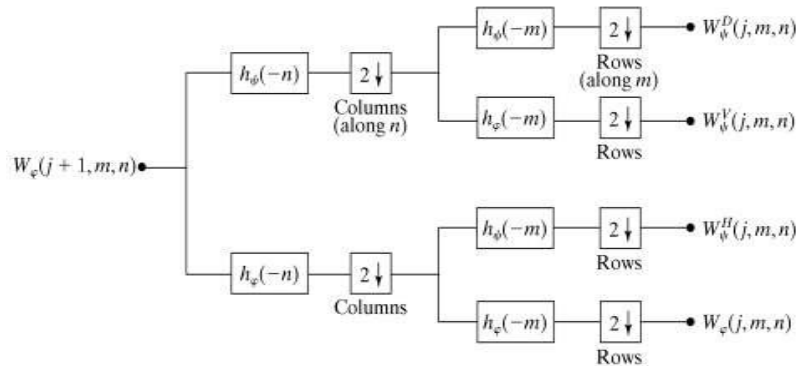


Figure 2.11 Two dimensional FWT ; analysis filter bank using QMF for image decomposition.

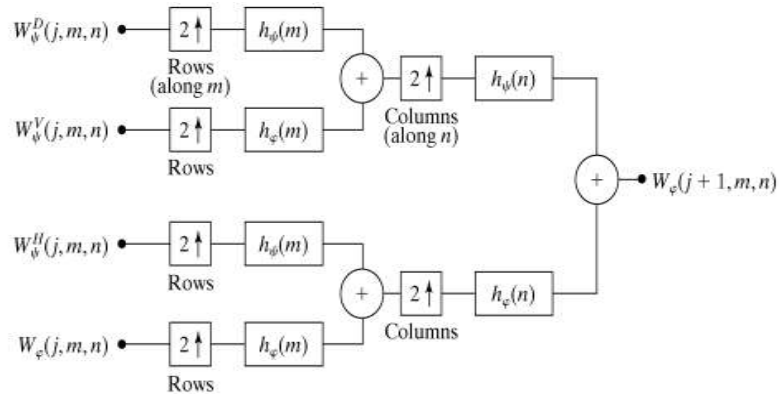


Figure 2.12 Image Synthesis using inverse QMF

Chapter 3

Novel Wavelet Synthesis for Image Compression and Entropy Reduction

3.1 Introduction

This part introduces a novel wavelet amalgamation approach in view of scale increase of concordant detail groups coefficients of dyadic wavelet change that smothers clamor in an image. The calculation takes a shot at default edge esteems for image compression. Anyway, to accomplish optimality of image compression and saving edges, level of image disintegration through wavelet change isn't one of a kind and relies on image goals alongside its auxiliary parameters. Scale controls the centrality of edges to be appeared. High goals images with thick edges bolster abnormal state decay and the other way around. The proposition displays a novel image compression worldview in which inventive wavelet blend of detail groups in light of bilinear addition and WSC is considered with the end goal that the recreated image manufactures a compressed image.

3.2 Image Compression Algorithm

Wavelet Synthesis Equations (2.77)- (2.80) are established wavelet disintegration conditions to discover the approximations and points of interest in two dimensional divisible signs[16]. Figure demonstrates the strategy created in this exploration: -

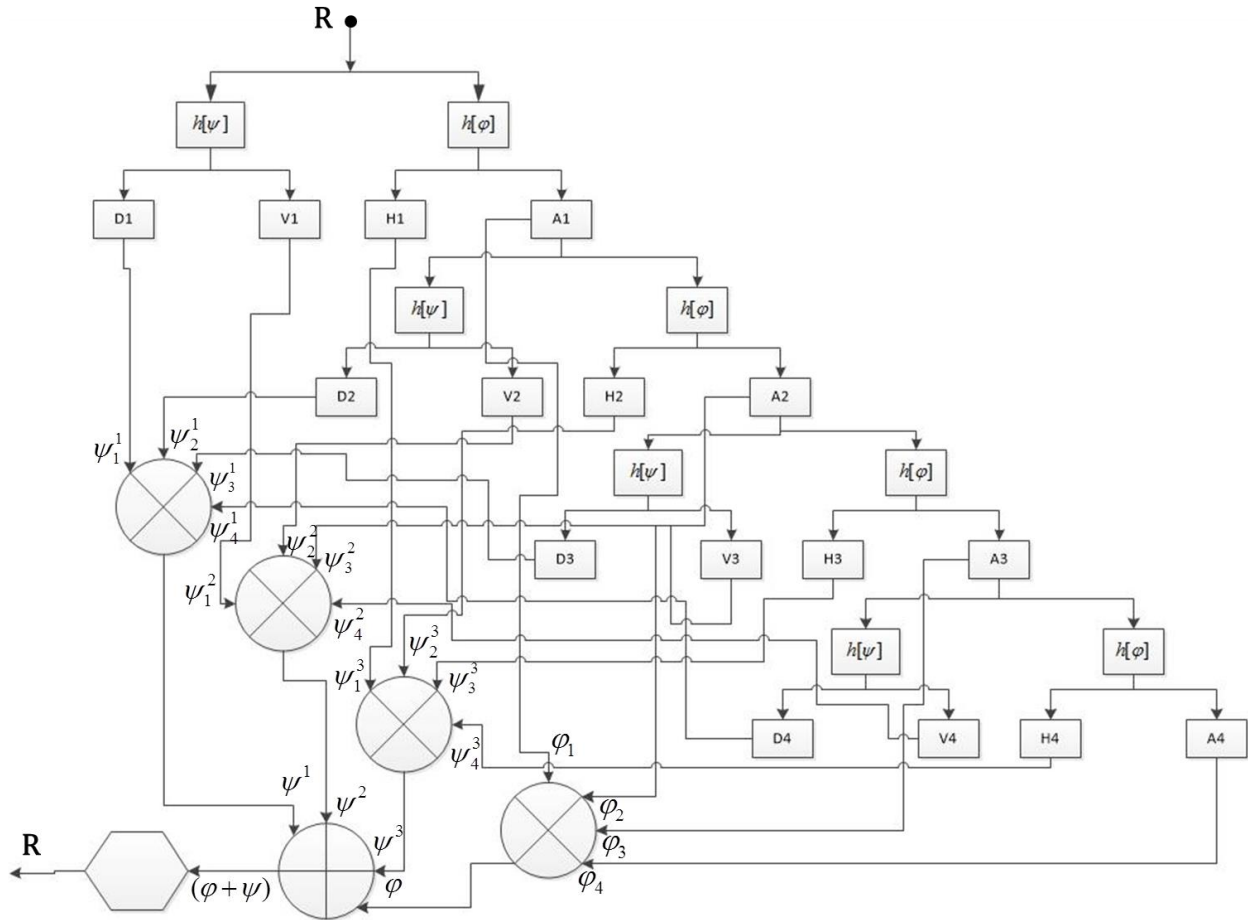


Figure 3.1 Figure 3.1 shows the wavelet investigation channel bank for the information image I taken after by its union channel bank for image compression for $n=4$. E is the resultant compressed image.

3.2.1 Wavelet synthesis

The image is gone through change examination channel bank that establishes two separate one dimensional changes. Right off the bat the image is separated along even pivot utilizing low pass and high pass examination channels that split image into two groups taken after by pulverization by two. The low pass channel relates to an

averaging task, removes the coarse data of the signal. The high pass channel compares to differencing task, separates the detail data of the image.



Figure3.2 Image Synthesis

At long last the image has been part into four groups i.e. approximations, even subtle elements, vertical points of interest and inclining points of interest and are signified by LL, HL, LH and HH separately as appeared in figure 3.13. The decay steps establish the level one or the primary scale disintegration. Image edge guide can be acquired in the lower goals by including all the detail groups. The handled image is returned to its unique measurement by up inspecting taken after by insertion. The detail groups are orchestrated to yield edge guide of the image. Anyway, for better edge vision the investigated detail groups are properly threshold before amalgamation to maintain a strategic distance from undesirable points of interest[13]. The LL band can be additionally decayed by emphasizing the comparable channel banks yielding second level disintegration and can be iterated additionally up to the admissible level giving nth level deterioration. This procedure is named as pyramidal disintegration of the image. The image is disintegrated in a chain of importance of goals, while considering increasingly goals layers, we get increasingly point by point take a gander at the image.

The interest of such a methodology [11] encourages maintenance of basic substance that may go undetected at one goals might be anything but difficult to spot at another which has been abused for edge discovery combined with commotion concealment. A couple of QMF is worked on dark level image in vertical taken after by even bearing[10], [12]. The wavelet disintegration of the image utilizing haar wavelet is appeared in figure beneath:

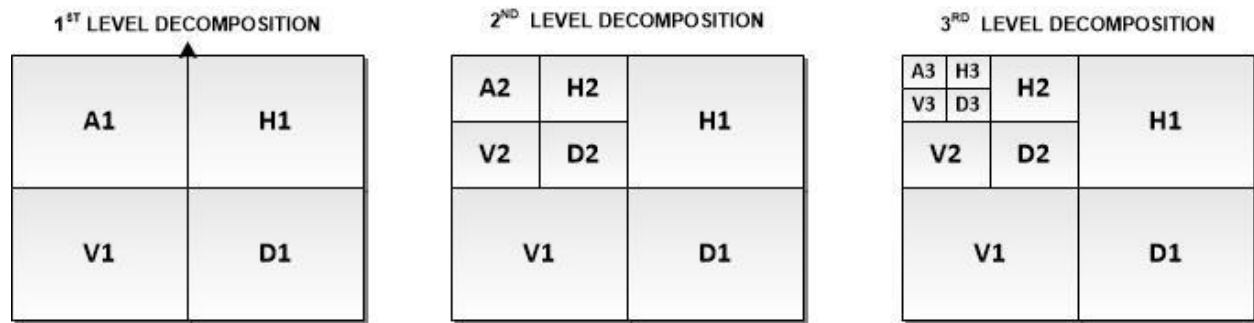


Figure 3.3 Image synthesis

To keep up the measure of the information at each level as for unique image, obliteration by two is connected after each sifting stage. High recurrence points of interest at each level are separated and used to get the size image of vertical and slanting image.

Lowpass deposit is taken for examination to get second, third and fourth level decay. Lowpass buildup is persisted from past level to repeat up to nth level. The disintegration level relies on image goals, structure, measurable parameters and edge thickness as talked about in past segment. The logical articulation for WSC image compression/entropy decrease is as per the following[8], [17]:

$$\psi^1 = \prod_{l=1}^n \psi_l^1 \quad (3.1)$$

$$\psi^2 = \prod_{l=1}^n \psi_l^2 \quad (3.2)$$

$$\psi^3 = \prod_{l=1}^n \psi_l^3 \quad (3.3)$$

$$\psi = \sum_{d=1}^3 \psi^d \quad (3.4)$$

$$E = n_{\sqrt{\psi}} = \left[\sum_{d=1}^3 \prod_{l=1}^n \psi_l^d \right]^{1/n} \quad (3.5)$$

Where ψ speaks to the blend of all the detail band coefficients by the given strategy, superscript $d=1,2,3$ speaks to interjected even, vertical and inclining subtle element groups to the first image estimate after duplication of concordant groups, subscripts l speaks to the decay level. E is the resultant edge guide of the image. The decay level n relies on the image goals, commotion power/model and its auxiliary parameters which incorporates the edge thickness, length and measurable parameters. The n th base of result of inserted estimate groups up to n th level is added to the edge identified image, it gives compressed image with decreased entropy:-

$$R = \phi + E \quad (3.6)$$

where R is the compressed reproduced image with decreased entropy. In the correct side of the condition, E has just been clarified in (3.1), (3.2), (3.3), (3.4), and (3.5). ϕ speaks to the estimation band introduced to unique image goals i.e.

$$\phi = \left(\prod_{l=1}^n \varphi_l \right)^{1/n} \quad (3.7)$$

the subscript l indicates the deterioration level. Be that as it may if the denoiser must be made in detachment and to conserve the circuit the approximations ought to be added preceding taking the n th root.

$$R = \left[\prod_{l=1}^n \varphi_l + \sum_{d=1}^3 \prod_{l=1}^n \psi_l^d \right]^{1/n} \quad (3.8)$$

3.2.2 Thresholding

In this calculation versatile thresholding is utilized to section the commotion pixels from the genuine information [8], [17]. In the least complex execution versatile thresholding regularly takes a grayscale image as info and the yield is a double image speaking to the division. In thresholding, an edge must be figured for every pixel in the image. In the event that the estimation of pixel under thought is over the estimation of edge ascertained it is set to the closer view esteem, else it expects estimation of the foundation[3].

Two fundamental methodologies are there for finding the limit, the Chow and Kaneko approach and Local thresholding. The two techniques depend on a similar supposition that littler image locales are typically more appropriate for thresholding as they are well on the way to have around uniform brightening. Chow and Kaneko system makes a variety of covering sub images by part a image, computing its histogram and by researching this histogram it ascertains the ideal edge for each sub image. At that point by interjecting the aftereffects of the sub images limit is found. However, this technique

has the disadvantage of being computationally costly and, thusly, it isn't reasonable for continuous applications.

An elective methodology for finding the nearby edge is to measurably inspect the power estimations of the nearby neighborhood of every pixel. These insights depend to a great extent on the info image and it ought to be generally fitting. Basic and quick capacities incorporate the mean of the neighborhood force conveyance. Adequate frontal area and foundation pixels must be secured so the extent of the area must be sufficiently substantial; generally, a poor edge is picked. In any case, by picking too huge areas, the supposition of around uniform brightening can be abused. The strategy we utilized is less computationally concentrated than the Chow and Kaneko approach and creates great outcomes.

In this strategy first the extent of pursuit window is chosen (here it is 10x10 window) and the mean of pixels and standard deviation is ascertained inside the window estimate, as there are sufficient closer view and foundation pixels inside the hunt window around every pixel along these lines the mean esteem lies between the power estimations of frontal area and foundation. To discover a limit the accompanying advances are performed right off the bat the window measure for averaging channel (mean) is chosen. At that point two limits are ascertained, one mean in addition to two standard deviation, and second in mean less two-standard deviation. The limit is chosen for every pixel when the estimation of a pixel is over the upper edge it is shrinked to the mean esteem; and when the esteem is beneath the lower edge it is likewise shrinked to mean esteem[7]. The outcome is an evacuation of uproarious pixels.

3.2.3 Interpolation

Due to down inspecting by a factor of two at each stage, the lower goals images are interjected up to unique size to encourage network duplication. At first closest neighborhood insertion was utilized yet it made pixilation impact. Later bilinear addition strategy was utilized which delivered great outcomes.

3.2.4 Matrix Multiplication

All grid increases are done at the first image goals. The event, vertical, askew and estimate inserted groups up to nth level are point insightful duplicated separately and the item detail groups are cumulated. The union of item groups if yielded at level one is re-interjected to coordinate the first size of the image. Anyway, it is helpful to introduce the item groups to the first size and afterward synthesize. The nth foundation of the cumulated detail band yields image edge delineates. The nth foundation of result of added estimation groups up to nth level is added to the edge identified image, it gives compressed image with lessened entropy[5].

3.2.5 Computational Complexity

The computational unpredictability for the remade image through WSC has been ascertained. The result of guess concordant band's intricacy is included by a factor of nN^2 . In this way the general computational multifaceted nature for image entropy decrease through WSC up to nth lvl utilizing Haar wavelet moves toward becoming:

$$N^2 \left\{ \left(\sum_{n=0}^l 2^{2(1-n)} + 4n + 1 \right) \right\} \quad (3.9)$$

Chapter 4

Results and Analysis

4.1 Introduction

Process of Discrete Wavelet Transform image compression has been performed to get the desired results. Efficacy of Image Compression Using Wavelet Transform in terms of qualities and robustness has been verified by performing several experiments on standard bench mark images. The performance of image quality and compression of reconstructed images have been compared. In this examination MATLAB R2008a was utilized for programming.

4.2 Input data

We have used standard gray image of Lena, cameraman and bird used in image processing as input data.

4.3 Experiment and Results

Following steps have been performed while compressing the image till reconstruction:-

4.3.1 Image having different resolutions have been loaded through computer and discrete wavelet transform has been applied using various wavelets. Image has been decomposed from level 1 to level 3.

4.3.2 An estimate of the original image has been reconstructed by applying the corresponding inverse transform.

4.3.3 Mean square error, peak signal noise ratio and compression ratio values for corresponding reconstructed images have been calculated.

4.3.4 Sample 1

Figure 4-1(a) to (c) show the result of proposed technique applied on a cameraman image of size 256 x 256



Figure 4-1 (a) Original Image of Resolution 256 x 256



Error Image



Reconstructed Image

Figure 4-1 (b) 1st Level Decomposed and Reconstructed Image



Error Image



Reconstructed Image

Figure 4-1 (c) 3rd Level Decomposed and Reconstructed Image

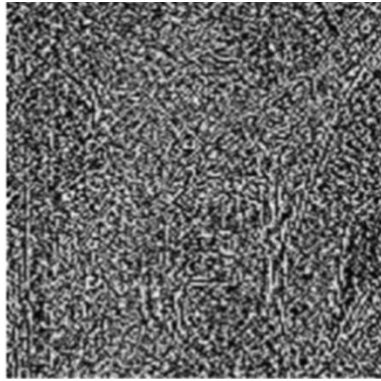
Values	1 st level decomposition		2 nd level decomposition		3 rd level decomposition	
	Threshold 10	Threshold 50	Threshold 10	Threshold 50	Threshold 10	Threshold 50
PSNR	40.79	30.67	39.74	30.24	39.37	29.17
Compression Ration	54.28	70.21	65.52	85.11	67.42	86.98

4.3.5 Sample 2

Figure 4-2(a) to (c) show the result of proposed technique applied on a Lena image of size 512 x 512



Figure 4-2 (a) Original Image of Resolution 512 x 512



Error Image



Reconstructed Image

Figure 4-2 (b) 1st Level Decomposed and Reconstructed Image



Error Image



Reconstructed Image

Figure 4-2 (c) 3rd Level Decomposed and Reconstructed Image

Values	1 st level decomposition		2 nd level decomposition		3 rd level decomposition	
	Threshold	Threshold	Threshold	Threshold	Threshold	Threshold
	10	50	10	50	10	50
PSNR	41.36	33.83	40.31	31.69	39.78	31.03
Compression Ration	62.01	73.29	72.59	89.41	73.89	92.33

4.3.6 Sample 3

Figure 4-3(a) to (c) show the result of proposed technique applied on a Parrot image of size 128 x 128



Figure 4-2 (a) Original Image of Resolution 128 x 128



Error Image



Reconstructed Image

Figure 4-3 (b) 1st Level Decomposed and Reconstructed Image



Error Image



Reconstructed Image

Figure 4-3 (c) 3rd Level Decomposed and Reconstructed Image

Values	1 st level decomposition		2 nd level decomposition		3 rd level decomposition	
	Threshold	Threshold	Threshold	Threshold	Threshold	Threshold
	10	50	10	50	10	50
PSNR	39.46	31.12	38.80	29.52	38.57	29.04
Compression Ration	56.11	71.81	66.81	86.07	68.39	89.51

4.4 Quality Metric

The people are the best judge for breaking down the image preparing applications, in this way psycho-visual examination is given due weight age. There exist different measures [18] that depend on brokenness in limit identification of various edges. The Mean Square Error (MSE) and the Peak Signal to Noise Ratio (PSNR) are the two mistake measurements used to look at image compression quality. The MSE speaks to the total squared mistake between the compressed and the first image, though PSNR speaks to a proportion of the pinnacle blunder. The lower the estimation of MSE, the lower the blunder[12].

$$MSE = \frac{\sum_{M,N}[I(m,n) - I_R(m,n)]^2}{M * N} \quad (4.1)$$

where I is the first image and IR is the compressed image and M*N is the aggregate number of pixels in the image. There are other conceivable decisions for assessing the nature of results, as there are signs that the mistake measures may not compare to best visual quality. Therefore, DT of the images has been misused. The supreme contrast from unique and uproarious image is taken as proportion of mistake. PSNR dependent on the DT is assessed as

$$PSNR = 10 \log_{10} \frac{R^2}{MSE} \quad (4.2)$$

where R is the pinnacle signal esteem which is 1 in the examinations. DT1 is the DT of the compressed image from unique image and DT2 is the DT of the edge distinguished image from uproarious image and their second standard is taken which is a scalar and figures their mean square mistake. In the event that m and n are the lines and sections of the DT lattice individually with the end goal that $dt_1(m,n) \in DT_1$ and $dt_2(m,n) \in DT_2$ then their second standard is characterized as segments of the DT grid separately to such an extent that $dt_1(m,n) \in DT_1$ and $dt_2(m,n) \in DT_2$ then their second standard is characterized as

$$\|DT_1 - DT_2\| \frac{2}{2} = \frac{1}{M \times N} \sum_m \sum_n |dt_1(m,n) - dt_2(m,n)| \quad (4.3)$$

The idea of Shannon's entropy assumes a focal job in data hypothesis and is in some cases alluded to as a proportion of vulnerability [16], [19]. Entropy H(x) of the edge delineate decided as

$$H(X) = \sum_i P(x_i) \ln(x_i) \quad (4.4)$$

where P(xi) is the likelihood of ith pixel esteem. The entropy gives the measure of data in the image. Anyway it is preposterous precisely to induce the entropy measure for edge guide of the image on the grounds that the entropy variety in the image because of commotion or data substance is a poorly presented issue. There exists no such realized strategy to surmise climate

the expansion or decline in entropy proportion of the image edge outline because of varieties in commotion thickness in the image or there exists genuine edges. Among various wavelet premise works, the entropy esteems acquired at ideal disintegration levels will be unique, which implies that their data substance will likewise be extraordinary. In this sense, the higher entropy esteem is the place more data is contained. Anyway the proposed measures supplement psychovisual examination. Recreated image utilizing haar wavelets for proposed calculation is contrasted and loud image of Lena with Gaussian clamor $N(0,0.04)$. Amazing outcomes are accomplished as appeared in figure 4.21 as far as entropy decrease and compression.

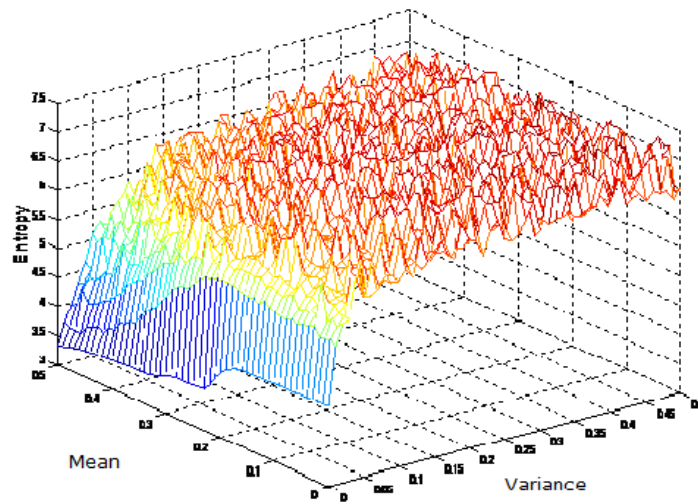


Figure 4.9 Entropy of the Proposed Image Denoiser

Lena image with counterfeit Gaussian clamor with changing mean and difference actuated is checked by the proposed calculation and its entropy is plotted utilizing (4.4) in figure 4.9. The entropy of the reproduced image is diminished significantly to one piece. Table 4.1 organizes image entropy and its reproduced image entropy for various clamor thickness in the image[11], [15].

CHAPTER 5

CONCLUSION AND FUTURE WORK

5.1 Conclusion

MRA has been explained and actualized on seat images. The smoothing abilities of wavelets combined with fine restriction of spatial space administrators have been abused to detail a HED that outflanked the established, recurrence area and wavelet-based administrators for default edge esteems. Adaptability for wavelets has been talked about and it is drawn out that the dimension of wavelet disintegration is the capacity of image goals, its basic parameters including factual parameters and the commotion level. The equivalent is utilized in image compression through WSC. The basic subtleties of the image stay present at all goals whereas commotion in the image is band constrained. This relationship in image structure at various goals is misused. A tale image compression channel is proposed by disintegrating the image through staggered wavelet deterioration utilizing QMF. The disintegration level is chosen dependent on its goals, measurable parameters and commotion level. At that point the dissected wavelet groups coefficients of the image are blended in such a way, to the point that the relationship with in subband is profoundly abused to yield compressed image. The incorporated image manufactures the compressed image. The excellence of calculation is that it works better for various images and commotions.

The outcomes have been assessed and looked at by abstract and in addition target examination. The psychovisual examination uncovers the matchless quality of the proposed plan which is increased by target investigation. Keeping in view the pixel's

delocalization amid denosing process, the blunder measures have been assessed utilizing DT. The images have been assessed utilizing entropy criteria. It is discovered that entropy of the compressed image of the proposed plan is diminished. PSNR of the compressed images have been determined and indicated impressive enhancement. The introduction in the proposed calculation reestablishes the frail edge pixels exhausted in the edge outline to thresholding. It works without the client's collaboration and can be exquisitely felt in pre-preparing stage for image compression and pressure. The remade image through scale connection effortlessly stifles clamor, lessens image entropy and supports further preparing in assorted applications, for example, image pressure or various depiction coding.

5.2 Limitations

Despite the fact that the calculation proposed in this examination has performed well for a few test images. It has a few requirements and confinements. The dimension of image deterioration at which the wavelet coefficients to be shrunk and broke down in not settle and depends totally on image goals. Bilinear insertion now and again does not create great outcomes when the image is up examined.

5.3 Future Work

When utilizing Wavelet Transform, the issue, for example, decision of essential goals (the scale level at which to start thresholding) and decision of investigating wavelet impact the achievement of the shrinkage methodology. The dimension of decay of the wavelet change and the decision of thresholding at a disintegration level to be investigated so that algorithm can viably be utilized for image compression and pressure. A superior introduction conspires be investigated for up sampling.

References

- [1] G. Kaur and R. Kaur, "Image De-Noising Using Wavelet Transform," vol. 2, no. 2, pp. 15–21, 2012.
- [2] S. M. Perumal and D. V. VijayaKumar, "A Wavelet Based Digital Watermarking method using Thresholds on Intermediate Bit Values," *Int. J. Comput. Appl.*, vol. 15, no. 3, pp. 29–36, 2011.
- [3] S. Claude, "A Mathematical Theory of Communication," *Bell Syst. Tech. J.*, vol. Vol.27, no. 1948, pp. 379–423, 1948.
- [4] M. A.-E. Abdou, "a Fuzzy Wavelet-Based Approach To a Novel Image Compression Engine," *Int. J. Comput. Appl.*, vol. 33, no. 4, 2011.
- [5] & Kulkarni, A.H. and A. P. R. K, "Applying image processing technique to detect plant diseases," *Int. J. Mod. Eng. Res.*, vol. 2, no. 5, pp. 3661–3664, 2012.
- [6] Basuki, "Analisis Data Penelitian Dengan Statistik," *Pengantar Kebijakan. Publik*, vol. 7581, no. 681, p. 87, 2006.
- [7] E. By, "International Journal of Image Processing," 2011.
- [8] U. W. Cse, "Lecture 3 Image Sampling, Pyramids, and Edge Detection."
- [9] P. Arbeláez, M. Maire, C. Fowlkes, and J. Malik, "Contour detection and hierarchical image segmentation.," *IEEE Trans. Pattern Anal. Mach. Intell.*, vol. 33, no. 5, pp. 898–916, 2011.
- [10] C. Chen, W. Wong, T. Lin, and C. Lin, "A novel wavelet-based multi-resolution skeleton extraction from a moiré image," no. May, 2014.

- [11] J. N and D. Suprava, "Automatic Image Registration Using Mexican Hat Wavelet, Invariant Moment, and Radon Transform," *Int. J. Adv. Comput. Sci. Appl.*, vol. 1, no. 1, pp. 75–84, 2013.
- [12] D. L. Donoho and I. M. Johnstone, "Adapting to unknown smoothness via wavelet shrinkage," *J. Am. Stat. Assoc.*, vol. 90, no. 432, pp. 1200–1224, 1995.
- [13] A. Mohammed and N. Hasan, "This electronic thesis or dissertation has been downloaded from the King ' s Research Portal at COGNITIVE RADIO NETWORKS ALI AL-TALABANI KING ' S COLLEGE LONDON."
- [14] S. Mallat, "A theory for multiresolution signal decomposition: the wavelet representation.," *IEEE Trans. Pattern Anal. Mach. Intell.*, vol. 11, no. 7, pp. 674–693, 1989.
- [15] R. S. Pathak, "Variation-Diminishing Wavelets and Wavelet Transforms," *Real Anal. Exch.*, vol. 37, no. 1, p. 147, 2017.
- [16] D. Heric and D. Zazula, "Adaptive Edge Detection with Directional Wavelet Transform," vol. 2005, pp. 1–4, 2005.
- [17] J. Wang, C. Wang, and T. Huang, "EFFICIENT IMAGE CONTOUR DETECTION USING EDGE PRIOR Beckman Institute , University of Illinois at Urbana-Champaign , USA Microsoft Research Asia , Beijing , China."